Structural Engineering and Mechanics, Vol. 17, No. 5 (2004) 671-690 671
DOI: http://dx.doi.org/10.12989/sem.2004.17.5.671

Development of a meshless finite mixture (MFM) method

J. Q. Cheng†, H. P. Lee‡ and Hua Li‡†

Institute of High Performance Computing, 1 Science Park Road, #01-01 The Capricorn, Singapore Science Park II, Singapore 117528

(Received July 18, 2003, Accepted December 22, 2003)

Abstract. A meshless method with novel variation of point collocation by finite mixture approximation is developed in this paper, termed the meshless finite mixture (MFM) method. It is based on the finite mixture theorem and consists of two or more existing meshless techniques for exploitation of their respective merits for the numerical solution of partial differential boundary value (PDBV) problems. In this representation, the classical reproducing kernel particle and differential quadrature techniques are mixed in a point collocation framework. The least-square method is used to optimize the value of the weight coefficient to construct the final finite mixture approximation with higher accuracy and numerical stability. In order to validate the developed MFM method, several one- and two-dimensional PDBV problems are studied with different mixed boundary conditions. From the numerical results, it is observed that the optimized MFM weight coefficient can improve significantly the numerical stability and accuracy of the newly developed MFM method for the various PDBV problems.

Key words: meshless method; finite mixture; point collocation; reproducing kernel particle; differential quadrature; least-square.

1. Introduction

The Finite Element Method (FEM) has been important numerical technique for a long time in modelling and simulation of engineering problems as the FEM has been proven to be highly effective for a wide range of engineering applications. However, the FEM has some drawbacks. For example, it requires the large computer memory due to the number of elements for complex problems and the iterative remeshing for tracking dynamic processes of large deformation problems. Therefore in the recent decade, the meshless approach, often referred to as the next-generation of numerical tool, has attracted much attention amongst researchers world-wide (Liu 2002). In general, meshless methods can be classified roughly into two groups. One requires a background mesh such as Galerkin-based techniques and reproducing kernel particle (RKP) method (Belytschko *et al.* 1994, Krongauz *et al.* 1996, Liu *et al.* 1995, 1996, Lu *et al.* 1994, Gunther and Liu 1998, Mukherjee and Mukherjee 1997, Hegen 1996, Zhu and Atluri 1998, Gosz and Liu 1996) and the other does not require a background mesh such as point collocation techniques (Gingold and Moraghan 1977, Onate *et al.* 1990, Liszka *et al.* 1996, Durate and Oden 1996). The latter

† PDF
‡ Associate Professor
‡† Principal Research Engineer

collocation-based techniques are true meshless methods, including the finite point method (Cheng and Liu 2002) and hybrid meshless-differential order-reduction (*h*M-DOR) method (Cheng *et al.* 2002, Ng *et al.* 2003) and the differential quadrature (DQ) method (Liu and Wu 2001, Shu 2000).

It is clear that each of the existing meshless approaches has its own special advantages. From the optimal viewpoint therefore, this paper proposes the finite mixture theorem to combine several existing meshless approaches as subcomponents for development of a new mehsless technique, named the meshless finite mixture (MFM) method. It fully takes the advantage of each existing meshless approach, where RKP and DQ methods are selected as two subcomponents and are mixed for approximate solution of unknown function. A weight coefficient for the mixture is optimized by the least-square technique. The formulations of the shape functions and their derivatives are carried out for the RKP and DQ methods. Then the point collocation technique is used to discretize the partial differential boundary value (PDBV) problems. Finally, the discretization PDBV system is solved numerically to determine the point value of the unknown function at the scattered points and the distribution of field function in the defined computational domain. Several numerical studies are conducted for one- and two-dimensional PDBV problems. The comparisons with exact solution are achieved well, which validate the presently developed MFM method.

2. Fundamental formulations of MFM method

2.1 RKP and DQ subcomponents

A finite mixture theorem is based on the concept that any one function can be composed of several subcomponents, within which the variables are homogeneous and between which the variables are heterogeneous. The weight coefficients incorporating the subcomponents are availably determined only by the variables themselves. The approximation $f_{mix}(x, y)$ of an unknown function $f(x, y)$ as a composite of the n subcomponents is thus written in the following form (Tarter and Lock 1994)

$$f_{mix}(x,y) = \alpha_1 f_1(x,y) + \alpha_2 f_2(x,y) + \ldots + \left(1 - \sum_{i=1}^{n-1} \alpha_i\right) f_n(x,y) \tag{1}$$

where α_i ($i = 1, 2, ..., n$) is the weight coefficient for the ith subcomponent with the requirements $0 < \alpha_i < 1$ and $\sum_{i=1}^{n} \alpha_i = 1$. f_i ($i = 1, 2, ..., n$) is the ith subcomponent and each subcomponent is different approximation function of the unknown function with different approximate error.

Based on the finite mixture theorem, the simplest case of the finite mixture model is to individualize only two subcomponents $f_1(x, y)$ and $f_2(x, y)$ to construct the mixture approximate function as follows

$$f_{mix}(x,y) = \alpha_1 f_1(x,y) + (1 - \alpha_1) f_2(x,y) \tag{2}$$

For development of the present meshless finite mixture (MFM) method, the existing RKP method is mixed with the DQ method to develop a truly meshless technique. The approximation $\tilde{f}_{mix}(x,y)$ of an unknown function $f(x, y)$ is thus generated as a mixture of the RKP and DQ approximations with weight coefficient α as follows

$$\tilde{f}_{mix}(x, y) = \alpha \tilde{f}_{RKP}(x, y) + (1 - \alpha)\tilde{f}_{DQ}(x, y) \tag{3}$$

or in the discrete form:

$$\tilde{f}_{mix}(x, y) = \alpha \sum_{i=1}^{N_p} N_i(x, y) f(x_i, y_i) + (1 - \alpha) \sum_{i=1}^{N_p} D_i(x, y) f(x_i, y_i) \tag{4}$$

where $\tilde{f}_{RKP}(x, y)$ is an approximation of the unknown function $f(x, y)$ by the reproducing kernel particle (RKP) method and $\tilde{f}_{DQ}(x, y)$ an approximation of the unknown function $f(x, y)$ by the differential quadrature (DQ) method. N_p is the total number of the scattered points in both the interior domain and boundary edges. $f(x_i, y_i)$ is the ith scattered point-value of the unknown function $f(x, y)$ to be determined. $N_i(x, y)$ and $D_i(x, y)$ are the shape functions constructed by the RKP and DQ methods (see late). α is the weight coefficient and is optimally determined to minimize the approximate errors by the least-square method, namely by constructing

$$J = \left[\alpha \sum_{i=1}^{N_p} N_i(x, y) f(x_i, y_i) + (1 - \alpha) \sum_{i=1}^{N_p} D_i(x, y) f(x_i, y_i) - f(x, y) \right]^2 \tag{5}$$

and having the stationary condition as,

$$\frac{\partial J}{\partial \alpha} = 0 \tag{6}$$

Thus two resulting equations are obtained as follows

$$\left[\sum_{i=1}^{N_p} N_i(x, y) f(x_i, y_i) - \sum_{i=1}^{N_p} D_i(x, y) f(x_i, y_i) \right] = 0 \tag{7}$$

or

$$\left[\alpha \sum_{i=1}^{N_p} N_i(x, y) f(x_i, y_i) + (1 - \alpha) \sum_{i=1}^{N_p} D_i(x, y) f(x_i, y_i) - f(x, y) \right] = 0 \tag{8}$$

In addition, the approximate truncation errors of the point-collocation-based RKP and DQ methods can be defined respectively:

$$E_{RKP}(f(x, y)) = \sum_{i=1}^{N_p} N_i(x, y) f(x_i, y_i) - f(x, y) \tag{9}$$

$$E_{DQ}(f(x, y)) = \sum_{i=1}^{N_p} D_i(x, y) f(x_i, y_i) - f(x, y) \tag{10}$$

Considering the definition Eqs. (9) and (10), Eq. (7) is rewritten as

$$\left[\sum_{i=1}^{N_p} N_i(x,y)f(x_i,y_i) - f(x,y)\right] - \left[\sum_{i=1}^{N_p} D_i(x,y)f(x_i,y_i) - f(x,y)\right] = E_{RKP}(f(x,y)) - E_{DQ}(f(x,y)) \tag{11}$$

Since $E_{RKP}(f(x,y))$ is not equal to $E_{DQ}(f(x,y))$, the first resulting Eq. (7) is impossible of existing. Therefore, the weight coefficient is obtained solely by the second resulting Eq. (8), i.e.

$$\alpha = \frac{f(x,y) - \sum_{i=1}^{N_p} D_i(x,y)f(x_i,y_i)}{\sum_{i=1}^{N_p} N_i(x,y)f(x_i,y_i) - \sum_{i=1}^{N_p} D_i(x,y)f(x_i,y_i)} \tag{12}$$

Furthermore, according to the definition of the approximate truncation errors expressed by Eqs. (9) and (10), Eq. (12) can be simplified as

$$\alpha = \frac{E_{DQ}}{E_{DQ} - E_{RKP}} \tag{13}$$

So far the formulation of meshless mixture finite (MFM) method has been completed. However, it is necessary to estimate the approximate truncation errors of the mixed subcomponents, the RKP and DQ methods, and to form the discrete expression of MFM approximation.

On the basis of the classical RKP method (Liu *et al.* 1995), an unknown real function $f(x, y)$ can be reproduced by integration with the chosen suitable kernel function $K(x_k - u, y_k - v)$ at a fixed central point (x_k, y_k) and the correction function $C(x, y, u, v)$ as

$$\tilde{f}_{RKP}(x,y) = \int_{\Omega} C(x,y,u,v)K(x_k-u, y_k-v)f(u,v)dudv \tag{14}$$

where $\tilde{f}_{RKP}(x,y)$ is a fixed reproducing kernel approximation of $f(x, y)$. It is also well known that any function can be extended as a series function in a fixed point by the Taylor series expansion. Thus the unknown function $f(x, y)$ is expanded at the point (0, 0) as follows

$$f(x,y) = f(0,0) + \left(x\frac{\partial}{\partial x} + y\frac{\partial}{\partial y}\right)f(0,0) + \ldots + \frac{1}{q!}\left(x\frac{\partial}{\partial x} + y\frac{\partial}{\partial y}\right)^q f(0,0) + \ldots$$
$$+ \frac{1}{(n+1)!}\left(x\frac{\partial}{\partial x} + y\frac{\partial}{\partial y}\right)^{n+1} f(\theta x, \theta y) \qquad (0 < \theta < 1) \tag{15}$$

where $f^N(\xi, \zeta)/\partial x^{N-n}\partial y^n$ is defined by

$$f^N(\xi,\zeta)/\partial x^{N-n}\partial y^n = \left.\frac{\partial^N f(x,y)}{\partial x^{N-n}\partial y^n}\right|_{\substack{x=\xi \\ y=\zeta}} \tag{15-1}$$

After substituting Eq. (15) into Eq. (14), the integral form of extended series for the RKP formulation is written as

$$\begin{aligned}\tilde{f}_{RKP}(x, y) = {} & f(0, 0)\int_{\Omega} C(x, y, u, v)K(x_k - u, y_k - v)dudv + \\ & + \frac{\partial f(0, 0)}{\partial x}\int_{\Omega} C(x, y, u, v)K(x_k - u, y_k - v)ududv + \\ & + \frac{\partial f(0, 0)}{\partial x}\int_{\Omega} C(x, y, u, v)K(x_k - u, y_k - v)vdudv + \ldots \\ & + \frac{1}{q!}\frac{\partial^q f(0, 0)}{\partial x^q}\int_{\Omega} C(x, y, u, v)K(x_k - u, y_k - v)u^q dudv + \ldots \\ & + \frac{1}{q!}\frac{\partial^q f(0, 0)}{\partial y^q}\int_{\Omega} C(x, y, u, v)K(x_k - u, y_k - v)v^q dudv \ldots \end{aligned} \tag{16}$$

Combining Eqs. (15) and (16) and rearranging, we have the resulting equation

$$\begin{aligned}\tilde{f}_{RKP}(x, y) - f(x, y) = {} & f(0, 0)\left[1 - \int_{\Omega} C(x, y, u, v)K(x_k - u, y_k - v)dudv\right] + \\ & + \frac{\partial f(0, 0)}{\partial x}\left[x - \int_{\Omega} C(x, y, u, v)K(x_k - u, y_k - v)ududv\right] + \\ & + \frac{\partial f(0, 0)}{\partial y}\left[y - \int_{\Omega} C(x, y, u, v)K(x_k - u, y_k - v)vdudv\right] + \ldots \\ & + \frac{\partial^q f(0, 0)}{\partial x^q}\left[x^q - \int_{\Omega} C(x, y, u, v)K(x_k - u, y_k - v)u^q dudv\right] + \ldots \\ & + \frac{\partial^q f(0, 0)}{\partial y^q}\left[y^q - \int_{\Omega} C(x, y, u, v)K(x_k - u, y_k - v)v^q dudv\right] + \ldots \end{aligned} \tag{17}$$

In order to obtain the discrete form of the approximation of the unknown function, usually a basic function $P(x, y)$ and correction function $\boldsymbol{C}(x, y)$ are introduced to replace the $C(x, y, u, v)$, Eq. (14) is thus rewritten as

$$\tilde{f}_{RKP}(x, y) = \int_{\Omega} P^T(u, v)C(x, y)K(x_k - u, y_k - v)f(u, v)dudv \tag{18}$$

Since the RKP method has the characteristics of consistency condition, the elements of the basic function $P(x, y)$ can be correctly reproduced by the integral form in terms of a suitable reproducing kernel $K(x_k - u, y_k - v)$. For instance, the nth-order basic function $P(x, y)$ may be in the following form,

$$P(x, y) = [1, x, y, \ldots\ldots x^n, x^{n-1}y, \ldots\ldots xy^{n-1}, y^n]^T \tag{19}$$

By consistency requirement (Liu *et al.* 1995), the elements of the basic function $P(x, y)$ are equivalently expressed in the following consistency conditions

$$1 = \int_{\Omega} P^T(u, v) C(x, y) K(x_k - u, y_k - v) dudv \tag{20-1}$$

$$x = \int_{\Omega} P^T(u, v) C(x, y) K(x_k - u, y_k - v) x dudv \tag{20-2}$$

$$y = \int_{\Omega} P^T(u, v) C(x, y) K(x_k - u, y_k - v) y dudv \tag{20-3}$$

$$\vdots$$

$$x^n = \int_{\Omega} P^T(u, v) C(x, y) K(x_k - u, y_k - v) x^n dudv \tag{20-i}$$

$$\vdots$$

$$x^{n-m} y^m = \int_{\Omega} P^T(u, v) C(x, y) K(x_k - u, y_k - v) x^{n-m} y^m dudv \tag{20-j}$$

$$\vdots$$

$$y^n = \int_{\Omega} P^T(u, v) C(x, y) K(x_k - u, y_k - v) y^n dudv \tag{20-k}$$

Substituting the above consistency condition Eq. (20) into Eq. (17), the truncation error of the RKP method is derived by

$$E_{RKP} = \|\tilde{f}_{RKP} - f\| \le C_3 a^n \|K'\|_{H^1} |f|_{W_\infty^{m+1}} \|\tilde{C}(a)\|_{H^1} \tag{21}$$

See Liu *et al.* (1996) for details.

By means of the RKP method with a fixed kernel approximation, Eq. (18) is discretizated in the form as

$$\tilde{f}_{RKP}(x, y) = \sum_{i=1}^{N_p} N_i(x, y) f(x_i, y_i) \tag{22}$$

where N_p is the total number of scattered points in both the internal domain and the boundary. For a regular distribution of N points along the x-axis direction and M points along the y-axis direction, $N_p = N \times M$. The shape function $N_i(x, y)$ developed by the RKP method with a fixed kernel approximation is written as Ng *et al.* (2003)

$$N_n(x, y) = \boldsymbol{B}(u_n, v_n) \boldsymbol{A}^{-1}(x_k, y_k) \boldsymbol{B}^T(x, y) K(x_k - u_n, y_k - v_n) \Delta s_n \tag{23}$$

For the subcomponent DQ method, it is necessary to compute the truncation error in 2-D formulation to estimate the weight coefficient in Eq. (13). Let us carry out the estimation of truncation error for a 1-D formulation first. In general, the 1-D truncation error of the DQ method is expressed by Shu (2000)

$$E_{DQ}(f(x)) = f^N(\xi)L(x)/N! \tag{24}$$

where ξ is a value of the variable x and N is the number of scattering points. $f^N(\xi)$ is presented as

$$f^N(\xi) = \left.\frac{\partial^N f(x)}{\partial x^N}\right|_{x=\xi} \tag{25}$$

and, $L(x)$ is defined as

$$L(x) = (x-x_1)(x-x_2)\ldots(x-x_N) \tag{26}$$

Then the estimation model of the 1-D truncation error is extended to the estimation of 2-D truncation error for DQ method. Based on the expression of 1-D truncation error (Shu 2000), the 2-D approximation $\tilde{f}(x,y)$ at fixed points x_i or y_j is expressed as

$$\tilde{f}(x,y_j) = \sum_{i=1}^{N} r_i(x)f(x_i,y_j), \qquad j = 1, 2, \ldots\ldots M \tag{27}$$

$$\tilde{f}(x_i,y) = \sum_{j=1}^{M} s_j(y)f(x_i,y_j), \qquad i = 1, 2, \ldots\ldots N \tag{28}$$

where N and M are the numbers of points scattered along the x-and y-axis directions respectively. $r_i(x)$ and $s_j(y)$ in Eqs. (27) and (28) are the Lagrange interpolation polynomials and given by

$$r_i(x) = \prod_{k=1, k\neq i}^{N} \frac{x-x_k}{x_i-x_k} \tag{29}$$

$$s_j(y) = \prod_{k=1, k\neq i}^{M} \frac{y-y_k}{y_i-y_k} \tag{30}$$

By Eqs. (27) and (28), the 2-D approximation of DQ method is developed as follows

$$\tilde{f}_{DQ}(x,y) = \sum_{i=1}^{N}\sum_{j=1}^{M} r_i(x)s_j(y)f(x_i,y_j) \tag{31}$$

Therefore, the definition of the 2-D approximate truncation error can be written as

$$E_{DQ}(f(x,y)) = f(x,y)-\tilde{f}(x,y) = f(x,y)-\sum_{i=1}^{N}\sum_{j=1}^{M} s_j(y)r_i(x)f(x_i,y_j) \tag{32}$$

Furthermore, the 2-D truncation errors along the x- and y-axis directions can be expressed respectively

$$E_{DQ}^{x}(f(x,y)) = f(x,y)-\sum_{i=1}^{N} f(x_i,y)r_i(x) \tag{33}$$

$$E_{DQ}^{y}(f(x,y)) = f(x,y)-\sum_{j=1}^{M} f(x,y_j)s_j(y) \tag{34}$$

By the 1-D expression Eq. (24) of the truncation error of DQ method, the above Eqs. (33) and (34) are rewritten as

$$E^x_{DQ}(f(x,y)) = f^N_x(\xi, y)L(x)/N! \tag{35}$$

$$E^y_{DQ}(f(x,y)) = f^M_y(x, \zeta)L(y)/M! \tag{36}$$

where $f^N_x(\xi, y)$, $f^M_y(x, \zeta)$, are defined in (15-1).

Finally, with the minimum of the approximate error, the 2-D approximate truncation error of DQ method is defined as

$$E_{DQ} = \max[E^x_{DQ}(f(x,y)), E^y_{DQ}(f(x,y))] \tag{37}$$

2.2 Implementation of the MFM method

To apply the MFM method for simulation of engineering application, it is required to generate the derivative approximation of the subcomponents of the MFM approximation. With a fixed kernel technique, the derivative approximation of the RKP subcomponent is written as follows:

$$\frac{\partial^n \tilde{f}_{RKP}(x,y)}{\partial x^n} = \sum_{i=1}^{N_p} \frac{\partial^n N_i(x,y)}{\partial x^n} f(x_i, y_i) \tag{38}$$

$$\frac{\partial^n \tilde{f}_{RKP}(x,y)}{\partial y^n} = \sum_{i=1}^{N_p} \frac{\partial^n N_i(x,y)}{\partial y^n} f(x_i, y_i) \tag{39}$$

$$\frac{\partial^n \tilde{f}_{RKP}(x,y)}{\partial x^{n-m}\partial y^m} = \sum_{i=1}^{N_p} \frac{\partial^n N_i(x,y)}{\partial x^{n-m}\partial y^m} f(x_i, y_i) \tag{40}$$

On the other hand, the 1-D derivative approximation of DQ subcomponent can be generally presented by

$$f_x^{(n-1)}(x_i) = \sum_{j=1}^{N} w_{ij}^{(n-1)} f(x_j) \tag{41}$$

$$f_x^{(n)}(x_i) = \sum_{j=1}^{N} w_{ij}^{(n)} f(x_j) \tag{42}$$

where the coefficient $w_{ij}^{(n)}$ is computed by

$$w_{ij}^{(n)} = n\left(w_{ij}^{(1)} w_{ii}^{(n-1)} - \frac{w_{ij}^{(n-1)}}{x_i - x_j}\right), \quad \text{for} \quad i \neq j \tag{43}$$

$$w_{ii}^{(n)} = -\sum_{j=1,\, i\neq j}^{N} w_{ij}^{(n)}, \quad \text{for} \quad n = 2, 3, \ldots, N-1, \quad \text{and} \quad i, j = 1, 2, \ldots, N \tag{44}$$

$$w_{ij}^{(1)} = \frac{M^{(1)}(x_i)}{(x_i - x_j)M^{(1)}(x_j)}, \quad \text{for} \quad i \neq j \tag{45}$$

$$w_{ii}^{(1)} = -\sum_{j=1,\, i \neq j}^{N} w_{ij}^{(1)} \qquad i, j = 1, 2, \ldots, N \tag{46}$$

with the definition of $M(x)$ and $M^{(1)}(x)$

$$M(x) = (x - x_1)(x - x_2)(x - x_3)\ldots(x - x_N)$$

$$M^{(1)}(x_k) = (x_k - x_1)(x_k - x_2)\ldots(x_k - x_{k-1})(x_k - x_{k+1})\ldots(x_k - x_{N-1})(x_k - x_N)$$

However, in order to combine the two subcomponents of the MFM method, the approximation $\tilde{f}_{DQ}(x, y)$ of the unknown function $f(x, y)$ of the DQ method is rewritten in the following 2-D form

$$\tilde{f}_{DQ}(x, y) = \sum_{i=1}^{N_p} D_i(x, y) f(x_i, y_i) \tag{47}$$

where $D_i(x, y)$ is obtained from Eq. (31). Therefore, based on the above merging technique, the 2-D derivative approximation of DQ subcomponent is given as

$$f_x^{(n)}(x_i, y_j) = \sum_{k=1}^{N} w_{ik}^{(n)} f(x_k, y_j) \tag{48}$$

$$f_y^{(m)}(x_i, y_j) = \sum_{k=1}^{M} w_{jk}^{(m)} f(x_i, y_k) \tag{49}$$

It is noted that the present MFM method employs local differential quadrature method (Zong and Lam 2002) to estimate the weight coefficient in terms of the above generalized differential quadrature. The main difference between the two different differential quadrature methods is the influence domain covered by the scattered points. The shape function of the generalized differential quadrature is based on the full domain along the x- and y-axis discreted by the Lagrangian interpolants. However, the shape function of the local differential quadrature method is based on the localized domain (Zong and Lam 2002).

According to the above discussion of the subcomponents and their derivatives, the derivatives of the MFM approximation with respect to x and y can be summarized as

$$\frac{\partial^n \tilde{f}_{mix}(x, y)}{\partial x^n} = \alpha \sum_{i=1}^{N_p} \frac{\partial^n N_i(x, y)}{\partial x^n} f(x_i, y_i) + (1 - \alpha) \sum_{i=1}^{N_p} \frac{\partial^n D_i(x, y)}{\partial x^n} f(x_i, y_i) \tag{50}$$

$$\frac{\partial^n \tilde{f}_{mix}(x, y)}{\partial y^n} = \alpha \sum_{i=1}^{N_p} \frac{\partial^n N_i(x, y)}{\partial y^n} f(x_i, y_i) + (1 - \alpha) \sum_{i=1}^{N_p} \frac{\partial^n D_i(x, y)}{\partial y^n} f(x_i, y_i) \tag{51}$$

$$\frac{\partial^n \tilde{f}_{mix}(x, y)}{\partial x^{n-m} \partial y^m} = \alpha \sum_{i=1}^{N_p} \frac{\partial^n N_i(x, y)}{\partial x^{n-m} \partial y^m} f(x_i, y_i) + (1 - \alpha) \sum_{i=1}^{N_p} \frac{\partial^n D_i(x, y)}{\partial x^{n-m} \partial y^m} f(x_i, y_i) \tag{52}$$

The above approximate expression of MFM method can be used to solve generic engineering PDBV problems, such as,

$$\boldsymbol{L}f(x, y) = P(x, y) \qquad \text{PDEs in computational domain } \Omega \tag{53}$$

$$f(x, y) = Q(x, y) \qquad \text{Dirichlet boundary condition on } \Gamma_D \tag{54}$$

$$\partial f(x, y)/\partial n = R(x, y) \qquad \text{Neumann boundary condition on } \Gamma_N \tag{55}$$

where $\boldsymbol{L}$ is a differential operator and $f(x, y)$ an unknown real function. By using the point collocation technique and taking $\tilde{f}(x, y)$ as the approximation of $f(x, y)$, the discretized approximation forms of the PDBV problem are given as

$$\mathbf{L}\tilde{f}_{mix}(x_n, y_n) = P(x_n, y_n) \qquad n = 1, 2, \ldots, N_\Omega \tag{56}$$

$$\tilde{f}_{mix}(x_n, y_n) = Q(x_n, y_n) \qquad n = 1, 2, \ldots, N_D \tag{57}$$

$$\frac{\partial \tilde{f}_{mix}(x_n, y_n)}{\partial n} = R(x_n, y_n) \qquad n = 1, 2, \ldots, N_N \tag{58}$$

where N_Ω, N_D and N_N are the numbers of scattered points in the interior computational domain and along the Dirichlet and Neumann edges, respectively, and the total number of scattered points is thus $N_T = (N_\Omega + N_D + N_N)$.

3. Numerical validation of the MFM method

To examine the accuracy and convergence of the present MFM method, numerical comparisons are carried out for several classical one- and two-dimensional partial differential boundary-value (PDBV) problems, including the 1-D Poisson equation with a forcing term and the 2-D Laplace equation with various mixed boundary conditions, for analysis of the effect of the weight coefficient on the numerical stability and accuracy of the developed MFM method. Using a refined version of the definition of the standard error, a global error measure ξ is defined (Mukherjee and Mukherjee 1997) for the present examination of numerical convergence,

$$\xi = \frac{1}{|f_{\max}|}\sqrt{\frac{1}{N_T}\sum_{i=1}^{N_T}(\tilde{f}_i - f_i)^2} \tag{59}$$

3.1 Convergence study

In order to study the convergence of the MFM method, a 1-D Poisson equation with a forcing term is considered here. The governing equation and the boundary conditions are given as

$$\frac{\partial^2 f}{\partial x^2} = 105x^2/2 - 15/2 \qquad -1 < x < 1 \tag{60}$$

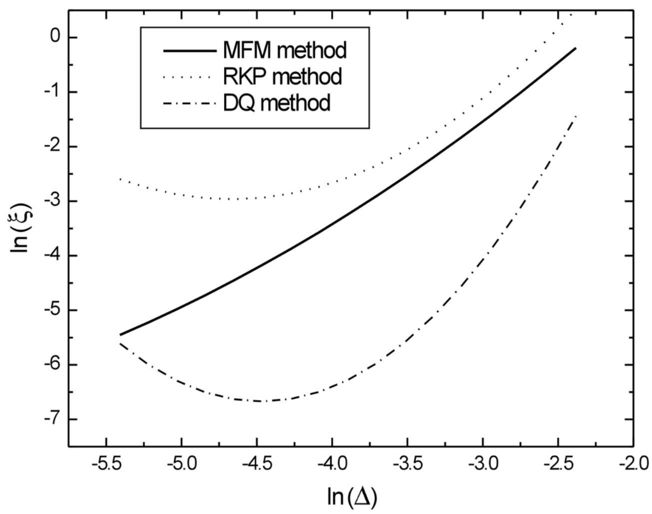

Fig. 1 Covergence of the MFM results for 1-D Laplace problem

$$f(x=-1) = 1 \tag{61}$$

$$\frac{\partial f}{\partial x}(x=1) = 10 \tag{62}$$

The exact solution of this problem is given by

$$f = \left(\frac{35}{8}\right)x^4 - \left(\frac{15}{4}\right)x^2 - \frac{3}{8} \tag{63}$$

By using the MFM method, the problem is solved numerically and the good convergence characteristic of the MFM method is depicted and confirmed in Fig. 1. For example, the global error is less than 5.06×10^{-3} for the 201 regular point distribution, when compared with the exact solutions. From the comparison among MFM method and subcomponents- RKP and DQ methods as shown in Fig. 1, it is clear that the numerical accuracy of RKP method is less than that of DQ method but its numerical stability is better than DQ's. As a mixture result of these subcomponent methods, MFM method can effectively mix and absorb the subcomponents' advantages, namely MFM method has a higher accuracy than RKP method and also has a better numerical stability than DQ method. These benefits of the MFM method can be further verified in the next numerical examples.

The second 1-D problem is the 1-D Poisson equation with a high localized gradient. The governing equation is

$$\frac{\partial^2 f}{\partial x^2} = -6x - \left[2/\phi^2 - 4\left(\frac{x-\beta}{\phi^2}\right)^2\right]\exp\left[-\left(\frac{x-\beta}{\phi}\right)^2\right] \tag{64}$$

and the boundary conditions

$$f(x=0) = \exp\left[-\left(\frac{\beta}{\phi}\right)^2\right] \tag{65}$$

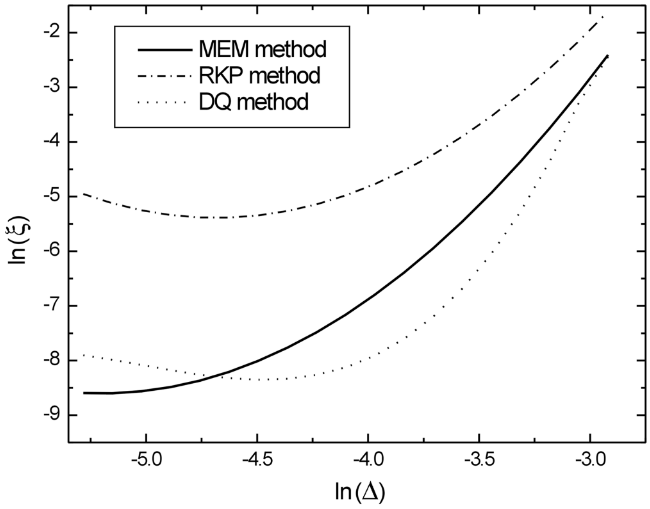

Fig. 2 Covergence of the MFM results for 1-D Poisson problem with a local gradient

$$\frac{\partial f}{\partial x}(x = 1) = -3 - 2\left(\frac{1-\beta}{\phi^2}\right)\exp\left[-\left(\frac{1-\beta}{\phi}\right)^2\right] \tag{66}$$

The exact solution is given by

$$f = -x^3 + \exp\left[-\left(\frac{x-\beta}{\phi}\right)^2\right] \tag{67}$$

Similarly, the developed MFM method is validated again and a good convergence characteristic is shown in Fig. 2. For example, the global errors for the 161 regular point distribution is smaller than 1.631×10^{-4}. With comparing to the RKP and DQ methods as shown in Fig. 2, it is found that the MFM method can really absorb the respective advantages of the subcomponent methods and obtain high and stable numerical results.

For a classical 2-D Laplace equation defined in a unit-square computational domain, the governing equation is given as

$$\frac{\partial^2 f(x,y)}{\partial x^2} + \frac{\partial^2 f(x,y)}{\partial y^2} = 0, \qquad 0 < x < 1 \quad \text{and} \quad 0 < y < 1 \tag{68}$$

The cubic-form exact solution of the given 2-D Laplace problem is presented by

$$f(x,y) = -x^3 - y^3 + 3xy^2 + 3x^2y \tag{69}$$

Four kinds of the pure or mixed boundary conditions are studied respectively. They are the pure Dirichlet boundary condition as shown in Fig. 3(a),

$$f(0,y) = -y^3, \quad f(1,y) = -1 - y^3 + 3y^2 + 3y \tag{70}$$

$$f(x,0) = -x^3, \quad f(x,1) = -x^3 - 1 + 3x + 3x^2 \tag{71}$$

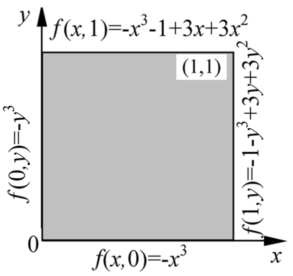

(a) Pure Dirichlet boundary condition.

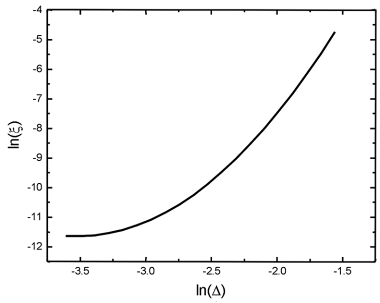

(b) Convergence for pure Dirichlet boundary condition.

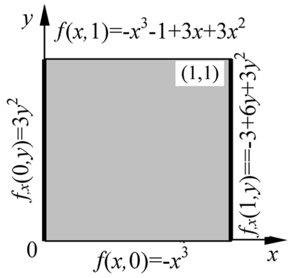

(c) Symmetrically mixed Dirichlet and Neumann boundary condition.

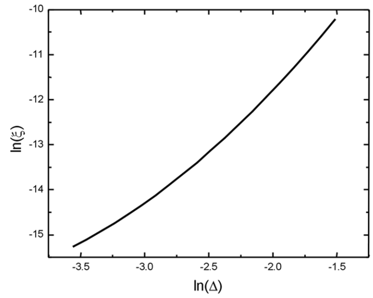

(d) Convergence for symmetrically mixed Dirichlet and Neumann boundary condition.

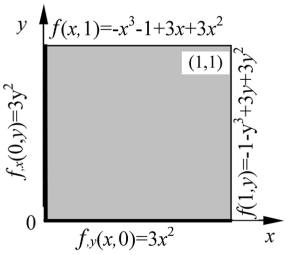

(e) Unsymmetrically mixed Dirichlet and Neumann boundary condition.

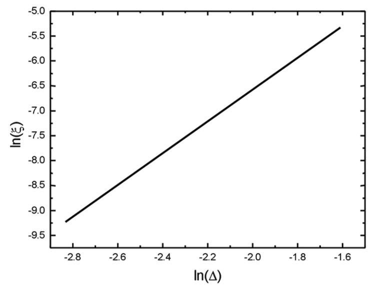

(f) Convergence for unsymmetrically mixed Dirichlet and Neumann boundary condition.

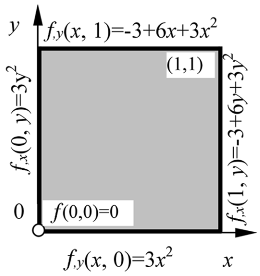

(g) Pure Neumann boundary condition.

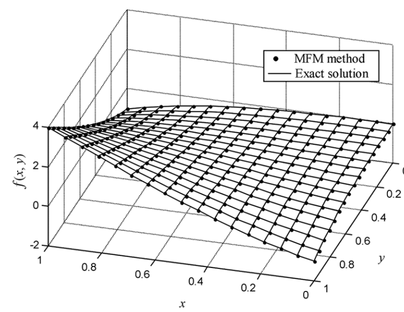

(h) Comparsion of pure Neumann boundary condition with exact solution

Fig. 3 Examination of the MFM method for the 2-D Laplace equation with various boundary conditions the symmetrically mixed Dirichlet and Neumann boundary condition as shown in Fig. 3(c)

$$f(x, 0) = -x^3, \quad f(x, 1) = -x^3 - 1 + 3x + 3x^2 \tag{72}$$

$$f_{,x}(0, y) = 3y^2, \quad f_{,x}(1, y) = -3 + 3y^2 + 6y \tag{73}$$

the unsymmetrically mixed Dirichlet and Neumann boundary condition as shown in Fig. 3(e)

$$f(x, 0) = 3x^2, \; f(x, 1) = -x^3 - 1 + 3x + 3x^2 \tag{74}$$

$$f_{,x}(0, y) = 3y^2, \quad f(1, y) = -1 - y^3 + 3y^2 + 3y \tag{75}$$

and the pure Neumann boundary condition as shown in Fig. 3(g)

$$f(0, 0) = 0.0; \; f_{,x}(0, y) = 3y^2; \; f_{,x}(1, y) = -3 + 3y^2 + 6y \tag{76}$$

$$f_{,y}(x, 0) = 3x^2; f_{,y}(x, 1) = -3 + 3x^2 + 6x \tag{77}$$

Using the developed MFM method, the numerical simulations for the above 2-D problems are solved and shown from Fig. 3. Figs. 3(b), 3(d) and 3(f) are achieved for examination of the MFM convergence characteristics. Fig. 3(h) shows the profiles of the numerical results and exact solution for the pure Neumann boundary condition. It is observed that the monotonic convergence trends demonstrate the numerical stability of the present MFM method. For example, for 17×17 regular point distribution, the global error of the MFM method for the pure Neumann boundary condition is smaller than 4.00×10^{-4}.

3.2 Effect of weight coefficient of the mixture

For discussion of the effect of weight coefficient α as a important feature of the presently developed MFM method, the steady-state heat conduction with a high gradient is considered in a 2-D rectangular plate with a heat source and the governing differential equation of the temperature field $T(x, y)$ is given by

$$\frac{\partial^2 T(x, y)}{\partial x^2} + \frac{\partial^2 T(x, y)}{\partial y^2} = -2s^2 \operatorname{sech}^2[s(y-0.5)]\tanh[s(y-0.5)]$$
$$0 < x < 0.5 \quad \text{and} \quad 0 < y < 1 \tag{78}$$

The boundary conditions are

$$T(x, y)|_{y=0} = -\tanh(s/2), \qquad T(x, y)|_{y=1} = \tanh(s/2) \tag{79}$$

$$\left.\frac{\partial T(x, y)}{\partial x}\right|_{x=0} = 0, \qquad \left.\frac{\partial T(x, y)}{\partial x}\right|_{x=0.5} = 0 \tag{80}$$

where s is a free parameter, and with increasing s, the field variable $T_{,y}(x, y)$ has an increasing gradient.

Table 1 Global errors of temperature T with different weight coefficients and point distributions for the high-gradient heat conduction by comparison with the exact solution (81)

Weight coefficient (α)	Different point distributions				
	3×51	3×101	3×151	3×201	3×241
1.0(RKP)	0.5112	0.1812	3.084E-2	9.520E-3	1.185E-2
8.0E-1	0.5114	0.1818	3.041E-2	7.396E-3	8.738E-3
5.0E-1	0.5116	0.1828	3.051E-2	4.914E-3	4.981E-3
1.0E-1	0.5119	0.1841	3.138E-2	3.637E-3	1.007E-3
0.0(DQ)	0.5120	0.1844	3.167E-2	3.780E-3	5.329E-4

Table 2 Global errors of temperature $T_{,y}$ with different weight coefficients and point distributions for the high-gradient heat conduction by comparison with the exact solution (82)

Weight coefficient (α)	Different point distributions				
	3×51	3×101	3×151	3×201	3×241
1.0(RKP)	0.1358	6.243E-2	2.440E-2	9.950E-3	5.3133E-3
8.0E-1	0.1357	6.127E-2	2.279E-2	8.737E-3	4.387E-3
5.0E-1	0.1356	6.000E-2	2.121E-2	7.523E-3	3.433E-3
1.0E-1	0.1355	5.887E-2	1.983E-2	6.567E-3	2.731E-3
0.0(DQ)	0.1355	5.867E-2	1.957E-2	6.403E-3	2.637E-3

For the above steady-state heat conduction problem with a high gradient located near $y = 0.5$, the exact solution of temperature field $T(x, y)$ is obtained as

$$T(x,y) = \tanh[s(y-0.5)] \tag{81}$$

and its first-order derivative with respect to y is

$$T_{,y}(x,y) = s \cdot \mathrm{sech}^2[s(y-0.5)] \tag{82}$$

By applying the present numerical MFM method to solve the above problem, the numerical results for the different weight coefficients are shown in Table 1 for the temperature $T(x, y)$ and Table 2 for its derivative $T_{,y}(x, y)$. It is clearly seen that the numerical MFM accuracy for both the temperature and its derivative can be improved by decreasing the weight coefficient with comparison with the point-collocation-based RKP method, but the computed MFM accuracy is less than that of the local DQ method. Fig. 4(a) is obtained for the comparison of the numerical results with the exact solution. For the convergence characteristics of the local gradient problem, Figs. 4(b) and 4(c) show the numerical results of the temperature $T(x, y)$ and its derivative $T_{,y}(x, y)$. As observed, a very good agreement is obtained with converged results. For example, for a 3×201 regular point distribution, the global errors of the MFM method is smaller than 3.64×10^{-3}. It is evidently revealed from Tables 1 and 2 and Fig. 4(c) that the better convergence characteristic of presently developed MFM method can be obtained by adjusting the weight coefficient within the region (0.0, 1.0) by comparing with the point-collocation-based RKP method. For the present problem, it is clearly indicated that the better numerical accuracy and stability can be obtained by the MFM method with the optimal weight coefficient $\alpha = 0.1$.

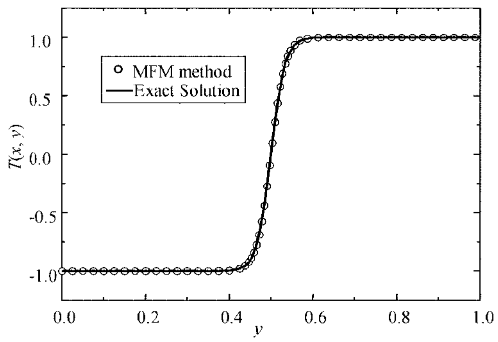

(a) Comparsion of the MFM method with exact solution.

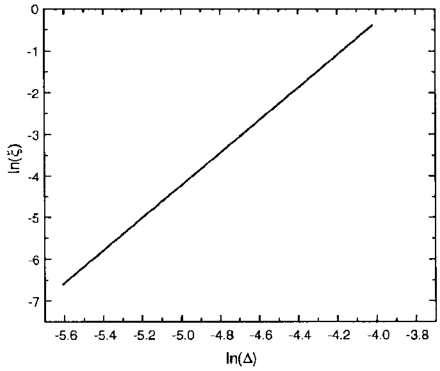

(b) Convergence characteristic of the MFM method results for the heat conduction problem.

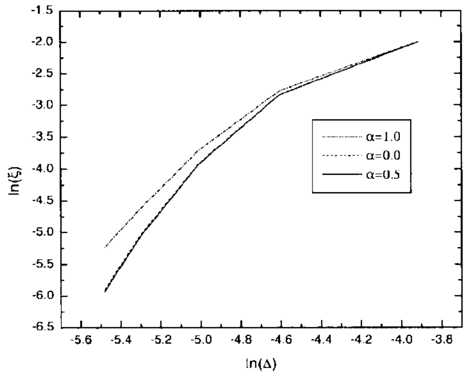

(c) Effect of the weight coefficient on the convergence of derivatives $f_{,y}$

Fig. 4 Numerical results and convergence characteristics of MFM method for heat conduction problem with a high gradient

The finally numerical study for analysis of the effect of weight coefficient α is a 2-D Poisson equation with a local high gradient in a unit-square computational domain

$$\frac{\partial^2 f(x,y)}{\partial x^2} + \frac{\partial^2 f(x,y)}{\partial y^2} = -6(x+y) - \frac{4}{a^4}(a^2 - (x-b)^2 - (y-b)^2)\exp\left[-\left(\frac{x-b}{a}\right)^2 - \left(\frac{y-b}{a}\right)^2\right]$$
$$0 < x < 1 \quad \text{and} \quad 0 < y < 1 \tag{83}$$

with the boundary conditions

$$f(x,y)|_{x=0} = \exp[-(b^2 + (y-b)^2)/a^2] - y^3 \tag{84}$$
$$f(x,y)|_{x=1} = \exp[-((1-b)^2 + (y-b)^2)/a^2] - (1+y^3) \tag{85}$$
$$f_{,y}(x,y)|_{y=0} = 2b\exp[-(b^2 + (x-b)^2)/a^2]/a^2 \tag{86}$$
$$f_{,y}(x,y)|_{y=1} = -3 - 2(1-b)\exp[-((x-b)^2 + (1-b)^2)/a^2]/a^2 \tag{87}$$

The exact solution of the given 2-D Poisson equation with a local high gradient is obtained as

$$f(x,y) = -(x^3+y^3)+\exp\left[-\left(\frac{x-b}{a}\right)^2-\left(\frac{y-b}{a}\right)^2\right] \tag{88}$$

and the first order derivatives of with respect to x- and y-direction are

$$f_{,x}(x,y) = -3x^2-\frac{2(x-b)}{a^2}\exp\left[-\left(\frac{x-b}{a}\right)^2-\left(\frac{y-b}{a}\right)^2\right] \tag{89}$$

$$f_{,y}(x,y) = -3y^2-\frac{2(y-b)}{a^2}\exp\left[-\left(\frac{x-b}{a}\right)^2-\left(\frac{y-b}{a}\right)^2\right] \tag{90}$$

It is seen that, if a and b are respectively taken to be 0.05 and 0.5, the local high gradient occurs near the centre point (0.5, 0.5) of the unit-square computational domain. Using the present MFM method, this problem is solved numerically and the simulation results for the different weight coefficients are shown in Table 3 for the function f and Table 4 and 5 for its derivatives $f_{,x}$ and $f_{,y}$. From the Tables 3-5, it is explicitly observed that the weight coefficients can adjust the numerical accuracy and stability of the MFM method, specially for their derivatives. Comparison of these numerical results with the exact solutions, the convergence characteristic for the function $f(x, y)$ and its derivatives are presented in Figs. 5(b-d) respectively. Excellent agreement is observed here and the global error in this example does not exceed 8.6×10^{-3} for the 21×21 regular point distribution.

Table 3 Global errors of function u with different weight coefficients and point distributions for the local high-gradient 2-D Poisson equation by comparison with the exact solution (88)

Weight coefficient (α)	Different point distributions			
	9×9	11×11	21×21	33×33
1.0(RKP)	1.730	0.9055	1.878E-2	2.426E-4
8.0E-1	1.715	0.8925	1.308E-2	4.245E-3
5.0E-1	1.717	0.8815	8.380E-3	2.438E-3
1.0E-1	1.728	0.8730	4.788E-3	5.695E-4
1.0E-2	1.730	0.8715	4.253E-3	2.644E-4
0.0(DQ)	1.730	0.8710	4.199E-3	5.755E-3

Table 4 Global errors of function $u_{,x}$ with different weight coefficients and point distributions for the local high-gradient 2-D Poisson equation by comparison with the exact solution (89)

Weight coefficient (α)	Different point distributions			
	9×9	11×11	21×21	33×33
1.0(RKP)	0.6772	0.3718	5.806E-3	5.678E-3
8.0E-1	0.6850	0.3757	3.217E-3	4.787E-3
5.0E-1	0.7000	0.3797	3.205E-3	3.851E-3
1.0E-1	0.7183	0.3841	4.287E-3	3.104E-3
1.0E-2	0.7217	0.3850	4.559E-3	2.999E-3
0.0(DQ)	0.7222	0.3850	4.588E-3	2.988E-3

Table 5 Global errors of function $u_{,y}$ with different weight coefficients and point distributions for the local high-gradient 2-D Poisson equation by comparison with the exact solution (90)

Weight coefficient (α)	Different point distributions			
	9×9	11×11	21×21	33×33
1.0(RKP)	0.3982	0.2397	5.772E-3	5.678E-3
8.0E-1	0.4054	0.2452	3.161E-3	4.787E-3
5.0E-1	0.4108	0.2505	2.963E-3	3.851E-3
1.0E-1	0.4148	0.2547	4.243E-3	3.104E-3
1.0E-2	0.4154	0.2554	4.517E-3	2.999E-3
0.0(DQ)	0.4156	0.2556	6.820E-3	2.998E-3

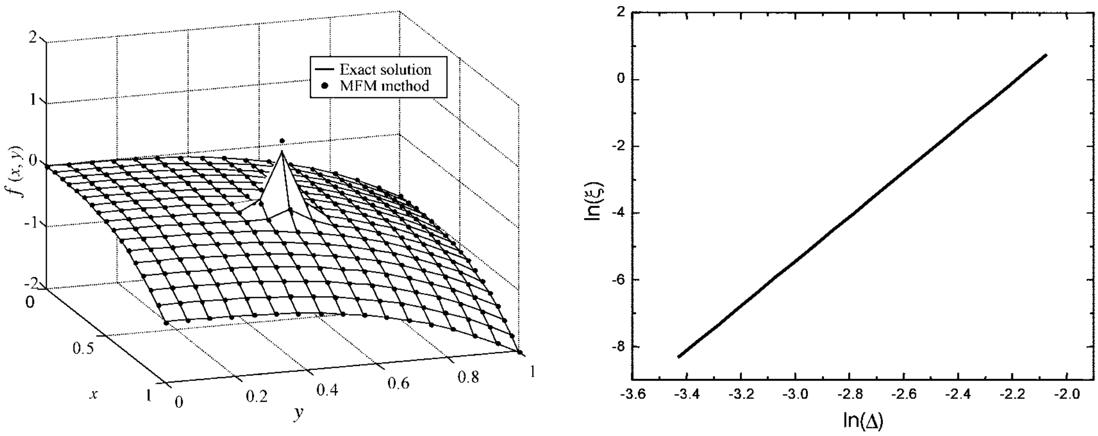

(a) Comparison of the MFM numerical results with the exact solution.

(b) Convergence characteristic of the MFM results.

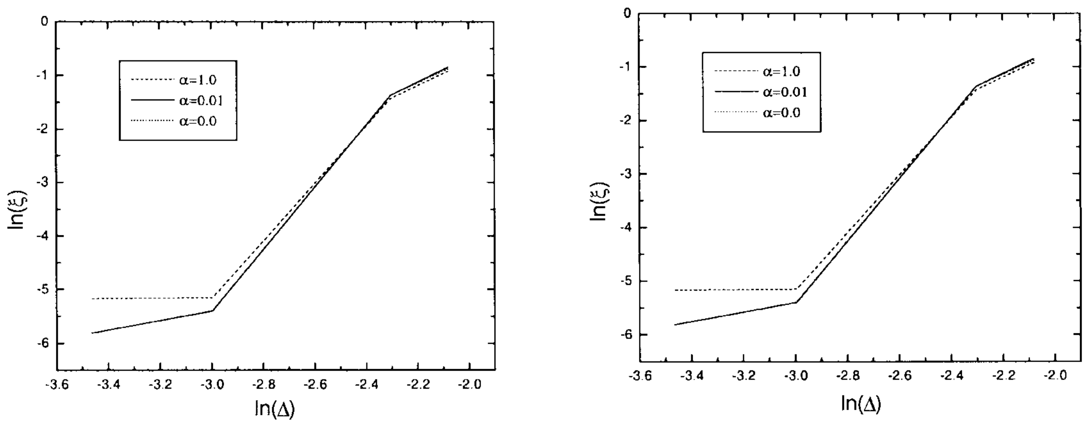

(c) Effect of the weight coefficient on the convergence of derivatives $f_{,x}$

(c) Effect of the weight coefficient on the convergence of derivatives $f_{,y}$

Fig. 5 Numerical results and convergence characteristics of MFM method for 2-D Poisson equation with a local high gradient

4. Conclusions

A new variation of point collocation based on the finite mixture theorem - the meshless finite mixture (MFM) method has been developed. It consists of a mixture of two existing meshless techniques as subcomponents - the classical reproducing kernel particle and differential quadrature methods to exploit the respective merits of these subcomponent techniques for the numerical solution of partial differential equations. In the presently developed MFM approximation, the weight coefficient is optimized by the least-square approach for higher numerical accuracy and stability. In order to examine the MFM method, convergence and weight coefficient studies have been carried out for various classical 1-D and 2-D examples. These studies clearly demonstrate the numerical stability and accuracy of the MFM method, and these appealing features can be attributed to the optimized weight coefficient derived within the MFM method.

References

Belytschko, T., Lu, Y.Y. and Gu, L. (1994), "Element free Galerkin methods", *Int. J. Numer. Meth. Eng.*, **37**, 229-256.

Cheng, M. and Liu, G.R. (2002), "A novel finite point method for flow simulation", *Int. J. Numer. Meth. Fluid*, **39**(12), 1161-1178.

Cheng, J.Q., Li, H., Lam, K.Y., Ng, T.Y. and Yew, Y.K. (2002), "A new hybrid meshless-differential order reduction (*h*M-DOR) method for deformation control of smart circular plate by distributed sensors/actuators", *Advances in Meshfree and X-FEM Methods*, Liu GR Editor, World Scientific Singapore, 49-54.

Duarte, C.A. and Oden, J.T. (1996), "An *h-p* adaptive method using clouds", *Comput. Meth. Appl. Mech. Eng.*, **139**, 237-262.

Gingold, R.A. and Moraghan, J.J. (1977), "Smoothed particle hydrodynamics: theory and applications to non-spherical stars", *Monthly Notices of the Astronomical Society*, **181**, 375-389.

Gosz, J. and Liu, W.K. (1996), "Admissible approximations for essential boundary conditions in the reproducing kernel particle method", *Comput. Mech.*, **19**, 120-135.

Gunther, F.C. and Liu, W.K. (1998), "Implementation of boundary conditions for meshless methods", *Comput. Meth. Appl. Mech. Eng.*, **63**, 205-230.

Hegen, D. (1996), "Element-free Galerkin methods in combination with finite element approaches", *Comput. Meth. Appl. Mech. Eng.*, **135**, 143-166.

Krongauz, Y. and Belytschko, T. (1996), "Enforcement of essential boundary conditions in meshless approximation using finite elements", *Comput. Meth. Appl. Mech. Eng.*, **131**, 133-145.

Liszka, T.J., Duarte, C.A.M. and Tworzydlo, W.W. (1996), "*hp*-meshless cloud method", *Comput. Meth. Appl. Mech. Eng.*, **139**, 263-288.

Liu, G.R. (2002), *Mesh Free Methods - Moving Beyond the Finite Element Method*, CRC Press.

Liu, G.R. and Wu, T.Y. (2001), "Application of generalized differential quadrature rule in Blasius and Onsager equation", *Int. J. Numer. Meth. Eng.*, **52**(9), 1013-1027.

Liu, W.K., Chen, Y., Chang, C.T. and Belytschko, T. (1996), "Advances in multiple scale kernel particle methods", *Comput. Mech.*, **18**, 73-111.

Liu, W.K., Jun, S. and Zhang, Y.F. (1995), "Reproducing kernel particle methods", *Int. J. Numer. Meth. Eng.*, **20**, 1081-1106.

Liu, W.K., Jun, S., Li, S., Adde, J. and Belytschko, T. (1995), "Reproducing kernel particle methods for structural dynamics", *Int. J. Numer. Meth. Eng.*, **38**, 1665-1679.

Lu, Y.Y., Belytschko, T. and Gu, L. (1994), "A new implementation of the element free Galerkin method", *Comput. Meth. Appl. Mech. Eng.*, **113**, 397-414.

Mukherjee, Y.X. and Mukherjee, S. (1997), "On boundary conditions in the element free Galerkin method", *Comput. Mech.*, **19**, 267-270.

Ng, T.Y., Li, H., Cheng, J.Q. and Lam, K.Y. (2003), “A new hybrid meshless-differential order reduction (*h*M-DOR) method with applications to shape control of smart structures via distributed sensors/actuators”, *Eng. Struct.*, **25**(2), 141-154.

Onate, E., Idelsohn, S., Zienkiewicz, O.C. and Taylor, R.L. (1990), “A finite point method in computational mechanics: applications to convective transport and fluid flow”, *Int. J. Numer. Meth. Eng.*, **39**, 3839-3866.

Shu, C. (2000), *Differential Quadrature and Its Application in Engineering*, Springer, Great Britain.

Tarter, M.E. and Lock, M.D. (1994), *Model-free Curve Estimation*, Chapman & Hall, New York.

Zhu, T. and Atluri, S.N. (1998), “Modified collocation method and a penalty formulation for enforcing the essential boundary conditions in the element free Galerkin method”, *Comput. Mech.*, **21**, 211-222.

Zong, Z. and Lam, K.Y. (2002), “A localized differential quadrature (LDQ) method and its application to the 2D wave equation”, *Comput. Mech.*, **29**, 382-391.